Pharm Res (2012) 29:1295–1307
DOI 10.1007/s11095-011-0643-y

RESEARCH PAPER

Magnetic Stents Retain Nanoparticle-Bound Antirestenotic Drugs Transported by Lipid Microbubbles

T. Räthel • H. Mannell • J. Pircher • B. Gleich • U. Pohl • F. Krötz

Received: 3 August 2011 / Accepted: 5 December 2011 / Published online: 22 December 2011

ABSTRACT

Purpose Coating coronary stents with antirestenotic drugs revolutionized interventional cardiology. We developed a system for post-hoc drug delivery to uncoated stents.

Methods We coupled rapamycin or a chemically similar fluorescent dye to superparamagnetic nanoparticles. The antiproliferative activity of rapamycin coupled to nanoparticles was confirmed *in vitro* in primary porcine vascular cells. The particles were then incorporated into lipid based microbubbles. Commercially available stents were made magnetizable by nickel plating and used to induce strong field gradients in order to capture magnetic microbubbles from flowing liquids when placed in an external magnetic field.

Results Nanoparticle bound Rapamycin dose dependently inhibited cell proliferation *in vitro*. Magnetic microcbubbles carrying coated nanoparticles were caught by magnets placed external to a flow-through tube. Plating commercial stents with nickel resulted in increased deposition at stent struts and allowed for widely increased distance of external magnets. Deposition depended on circulation time and velocity and distance of magnets. Deposited microbubbles were destroyed by ultrasound and delivered their cargo to targeted sites.

Conclusions Drugs can be incorporated into nanoparticle loaded microbubbles and thus be delivered to magnetizable stents from circulating fluids by applying external magnetic fields. This technology could allow for post-hoc drug coating of already implanted vascular stents.

KEY WORDS coronary stent · magnetic targeting · microbubble · nanoparticles · restenosis

INTRODUCTION

The implantation of stents into critically narrowed coronary arteries has become the standard treatment for ischemic coronary heart disease since the mid-nineties. The early success of stenting, however, has been hampered by two major limitations: one is the risk of uncontrolled platelet aggregation at the stent, ultimately leading to a so-called "in stent thrombosis", which is treated using antiplatelet substances. A second is the late recurrence of narrowing within the stent, the so-called "in-stent restenosis". In the two 1994 landmark studies for coronary stenting, in-stent restenosis occurred in 20–30% of patients (1,2). The introduction of stents that release antiproliferative drugs from their struts has dramatically reduced the problem of stent restenosis. The first of these drug-eluting stents (DES) released either rapamycin or paclitaxel (3). Today, DES of the second or third generation, releasing rapamycin-derivatives, are standard for treating stenosed coronaries (4). Rapamycin and its derivatives have proven superior to paclitaxel because of lower rates of late stent thrombosis. Restenosis in modern

T. Räthel · H. Mannell · J. Pircher · F. Krötz
Cardiology, Medical Policlinic, University Hospital Munich
Ziemssenstrasse 1
Munich, Germany

U. Pohl
Walter-Brendel Centre, Institute for Experimental Medicine
Ludwig-Maximilians-University
Schillerstrasse 44
80336 Munich, Germany

B. Gleich
Institute of Medical Engineering, Technical University Munich
Boltzmannstr. 11
85748 Munich, Germany

F. Krötz (✉)
Department for Invasive Cardiology, Medical Clinic, Starnberg Hospital
Oßwaldstr. 1
82319 Starnberg, Germany
e-mail: f.kroetz@klinikum-starnberg.de

DES still occurs but its rates are decreased to ~3–20% (4). The timeframe for the development of restenosis varies from weeks to months and is highly individual from patient to patient. It depends mainly on the reconvalescence of the vascular integrity of the stented site and is not predictable from the time point of the intervention (5–7). Drug coated stents, however, release their load within a few weeks. Thus, the quest for new strategies to transfer antirestenotic drugs to stents has evolved to extend and individualize pharmacological treatment. One resulting strategy was the development of drug-eluting balloons (DEB) (8). These DEB carry paclitaxel and are deployed in a coronary artery for 30 s, an interval, during which the substance is intended to be deposited to the target lesion. However, the DEB technology has several disadvantages: for one, although this would have been desirable, rapamycin or its derivatives could not be used to coat balloons for targeted transfer due to technological reasons. In addition, a second invasive catheterization procedure with prolonged times of balloon inflation and subsequent artificial induction of vessel ischemia is needed to deploy the substance. Moreover, although several balloons that carry paclitaxel have been developed, only a limited number has proven clinically effective (9).

Therefore, alternative methods to transfer antirestenotic drugs, preferentially rapamycin, to restenosed stents would be of great clinical interest. In this study, we tested the hypothesis, whether magnetic nanoparticle assisted targeting of rapamycin to stents is feasible. To address this question, we developed a drug delivery system which consists of three main steps: 1. coupling or associating the drug to nanoparticles and subsequent incorporation of drug coated particles into lipid microbubbles, 2. collecting the microbubbles to the target site by magnetic force and 3. destroying deposited microbubbles by ultrasound thereby depositing their load at the target site, thus generating a depot of pharmacologically active substances at the stent struts. One hurdle to overcome in magnetic targeting *in vivo* is the limited realization of sufficient magnetic field gradients in deeper areas of the body, such as coronary vessels. A second topic evolving with magnetic targeting of drug delivery systems is the target specific deposition of carrier systems, as the tissue surrounding the target site is also steeped with the magnetic field. We therefore adapted a previously described concept of using magnetizeable stents that may exert field modulating properties when exposed to an external magnetic fields (10,11), thus allowing for sufficient field gradients in greater distances of an external magnet. As a second feature, field forces can be chosen in a sufficient strength so that magnetic moments are only strong enough for particle deposition at the close proximity of the magnetizeable stent. Magnetic moments of superparamagnetic particles depend on their size which, however, is limited in vascular drug delivery. To increase magnetic moments and additionally reduce deposition of nanoparticle bound substances at unintended sites, we aimed to combine the magnetic targeting of rapamycin with the microbubble technology. Flexible lipid microbubbles assembling many nanoparticles exhibit greater magnetic moments than single particles concurrently owing perfect characteristics for the circulation in the vascular system.

MATERIALS AND METHODS

Chemicals

Lipids for microbubble formulation had pharmaceutical grade quality and were purchased from Lipoid GmbH (Ludwigshafen, Germany). Super paramagnetic iron oxide nanoparticles with individual coatings were a kind gift of Dr. Christian Bergemann, chemicell GmbH (Berlin, Germany). The Particles we used were either uncoated (FluidMAG-UC/C), coated with rapamycine (FluidMAG-Rapamycin, 1 mg per 10 mg iron oxide particles), or coated with the fluorescent dye perylene (FluidMAG-FG) as a model compound with physicochemical properties similar to rapamycine. The particles were especially developed for drug delivery in this project. All other Lab chemicals were purchased from Sigma-Aldrich (Taufkirchen, Germany).

Stents and Magnets

As a model for magnetizable coronary stents a commercially available cobaltchromium stent (Coroflex® Blue, 4 mm × 25 mm, BBraun, Melsungen, Germany) was expanded and subsequently nickel plated (Galvanische Werkstätten Heinrich Beer GmbH, Munich, Germany) to provide sufficient magnetic properties. For retention experiments, strong round neodymium permanent magnets (Ø 20 mm × 10 mm or Ø 25 mm × 6 mm) were used. The magnets were purchased from IBSMagnet (Berlin, Germany) and had a residual magnetism of 1.2 T.

Cell Culture

Porcine aortic endothelial cells (PAEC) and Porcine vascular smooth muscle cells (PVSMC) were isolated from fresh bovine aortas. For isolating PAEC, the aortas were cleaned from adherent tissue, cut longitudinally and washed in phosphate buffered saline (PBS). The rinsed aortas were clamped in a suitable device and the endothelium incubated for 1 h at 37°C with 0.2 U/ml collagenase A (Roche Diagnostics Deutschland GmbH, Mannheim, Germany) in Hank's buffered saline solution. Following incubation, some cell culture medium was added and the endothelial cells detached with a cell scrapper. Cell suspension was collected

and centrifuged at 1200 rpm for 5 min, the supernatant was removed and the cell pellet resuspended in fresh cell culture medium. Then cells were plated to 10 cm cell culture dishes. Culture medium was changed after about 6 h when cells were adherent to cell culture dishes and cells cultivated to confluence. Subsequent cell culture followed standard cell culture procedures. Cells were used from passage 3 to 15.

For isolation of PVSMC, the deendothelialized remainders of the porcine aortae were used. First, remaining endothelial cells were removed carefully by scratching the endothelial side of aortas with a scalpel. Then the aortic tissue was cut into pieces of 5 mm×5 mm and put into a 10 cm cell culture dish with the luminal side downwards. They were then incubated for 4 h at 37°C with 0.2 U/ml Collagenase A in Hank's solution. Subsequently, the collagenase solution was removed and cell culture medium added. Medium was changed every 3 days. After a sufficient amount of cells had sprouted out from the tissue patches, patches were removed and the smooth muscle cells' identity verified by immunostaining for smooth muscle actin. Following these procedure, cells were cultivated following standard cell culture procedures. Cells were used for experiments between passages 4 to 15.

All cells were cultured in Dulbeccos Modified Eagles Medium with phenol red (DMEM, Sigma-Aldrich, Taufkirchen, Germany) supplemented with 1 g/L glucose, 2 mM L-Glutamine, 10% bovine serum and penicillin/streptomycin (Sigma-Aldrich, Taufkirchen, Germany) at a final concentration of 100 U/ml penicillin and 100 µg/ml streptomycin.

MTT Assay

Cell viability was measured by the ability of living cells to reduce Methylthiazoletetrazolium, MTT, (0.5 mg/ml, 2 h) to formazan salt as described before (12). For viability measurements, cells were washed with PBS^+ and incubated with 0.5 mg/ml MTT in DMEM without phenol red for 2 h. Cells were then washed with PBS^+ and 100% Isopropanol was applied to the cells. The absorbance of the solution was measured at 550 nm and 620 nm in a plate reader (Tecan Spectra Fluor, Tecan, Crailsheim, Germany). The 620 nm value was substracted from the 550 nm value to exclude possible cell debris. Data were set in relation to non treated cells.

Preparation of Magnetic Microbubbles

For 1 ml of microbubble solution, dipalmitoylphosphatidylethanolamine (DPPE) and dipalmitoylphosphatidylcholin (DPPC) in different proportions were mixed in chloroform in a round bottom flask using rotation under heating at 60°C in a water bath. The organic solvent was then removed under vacuum using a Rotavapor-R (Büchi Labortechnik GmbH, Essen, Germany) and the remaining lipid mixture was suspended in 10% glycerol at 60°C in a water bath under rotation. 250 µg magnetic iron oxide nanoparticles were mixed with 1 ml of the lipid suspension in 1.5 ml glass vials with screw caps with silikon/PTFE membranes (Schubert & Weiss Omnilab GmbH, München, Germany). The mixture was then covered with perfluorpropane gas and shaken for 20 s in a CapMix (3 M ESPE, Seefeld, Germany). The formation of microbubbles was confirmed by microscopy and by applying pressure to the mixture forcing the micobubbles to burst leaving a clear solution. The incorporation of superparamagnetic nanoparticles coated with perylene to microbubbles was controlled by fluorescence microscopy (Axiovert 200 M microscope, Zeiss, Jena, Germany).

Retention of Magnetic Microbubbles in Flow Experiments

A transparent teflon tube with an inner diameter of 4 mm, either stented or without a stent was connected via flexible tubes to a liquid reservoir and a peristaltic pump (MS Reglo, Ismatec Laboratoriums GmbH, Wertheim, Germany). The tube was placed in a transparent acrylic glass cube with cavities to adequately place two permanent magnets in a defined distance at each side of the tube. A distance of 10 mm between the two applied permanent magnets resulted in a magnetic flux density of 0.3 T with the 25 mm magnets and of 0.4 T with the 20 mm magnets respectively at the axes of the stented tube. The suspension of magnetic microbubbles (1 ml of bubble suspension freshly prepared as described above diluted to 10 ml with pure water) was placed in the reservoir and pumped through the test tube with a velocity of 5 cm/s (pump speed 75, calculated from the tube diameter and the measurement of the liquid volume forced through the tube in a defined time). Pictures were taken from the experimental setup before and after circulating the suspension of the microbubbles through the test tube with a commercial digital camera. In some experiments, the permanent magnets were carefully removed without moving the deposited magnetic material before taking the photographs to obtain better sight on the situation within the tube. In other cases the tube was carefully removed from the experimental setup and the deposited perylene bearing magnetic nanoparticles were made visible by fluorescence microscopic imaging.

Quantification of Nanoparticle-Drug Complex Deposition at the Stent

A suspension of magnetic microbubbles was pumped through the experimental setup (see corresponding figures). After the intended deposition time the peristaltic pump was stopped and the deposited bubbles destroyed at the stented

site of the test tube by the application of ultra sound (Richmar Semitron, Richmar, Inola, USA) of 1 MHz, 2 W/cm^2 at 50% duty cycle for 30 s. Then, the stented tube was carefully removed from the experimental setup without losing magnetic material. The retained iron oxide particles were spilled from the tube into a defined volume of Methanol. The transported perylene was dissolved from the particles to methanol by placing the suspension in an ultrasound bath for a few minutes. After the solving procedure, the iron oxide particles were removed from the perylene solution by placing it onto a permanent magnet for a sufficient time. Subsequently, the supernatant was collected and the fluorescence was quantified by absorption measurement at 470 nm in a spectrophotometer (Shimadzu UV 1602, Shimadzu Deutschland GmbH, Duisburg, Germany). The amount of deposited material was calculated from a calibration curve obtained from different concentrations of FluidMAG-FG in Methanol treated as described.

Statistics

Statistical analyses were performed by analysis of variances (ANOVA) followed by a Bonferoni multiple comparison test or Dunn's post hoc test and calculated using SigmaStat 3.10 (Systat Software Inc., Chicago, USA).

RESULTS

Rapamycin Bound to Superparamagnetic Iron Oxide Nanoparticles Maintains Antiproliferative Characteristics

To prove that active pharmaceutical compounds still exhibit pharmacological action after coating to particles, we applied rapamycin laminated nanoparticles to cells in culture and compared their effect on cellular proliferation to free rapamycin as a control. The preparation of rapamycin coated nanoparticles contained 1 mg rapamycin per 10 mg of iron oxide particles. The particles were provided as a suspension in pure water with a concentration of 10 mg/ml, so that a dilution of 1:10,000 in cell culture medium corresponds to a final concentration of about 100 nM rapamycin. Rapamycin bound to iron oxide nanoparticles at a dilution of 1:10,000 inhibited cell proliferation of porcine aortic endothelial cells (PAEC) completely and the proliferation of porcine vascular smooth muscle cells (PVSMC) by 31%. The same concentration of free rapamycin added to cell culture medium resulted in complete inhibition of proliferation in PAEC and decreased the PVSMC proliferation by 36% (n=3 each). Uncoated nanoparticles had no comparable effect (see Figs. 1 and 2).

Lipid Suspensions Mixed with Superparamagnetic Nanoparticles Form Stable Gas-Filled Lipid Microbubbles

Using our especially developed lipid mixture suspended in water/10% glycerine (Fig. 3a) we were able to produce stable perfluorcarbon gas filled lipid microbubbles, which readily bound superparamagnetic iron oxide nanoparticles. The microbubbles bound both naked magnetic nanoparticles as well as rapamycin or otherwise coated magnetic nanoparticles. The microbubbles floated to the surface of the solvent when allowing the dispersion to stand for a while after bubble generation but could easily be redispersed by slightly shaking the vial (Fig. 3b and c). In order to demonstrate the binding of iron oxide particles and subsequent magnetizability of microbubbles, we placed a strong permanent magnet at one side of the vial. As demonstrated in Fig. 3d, the magnetic microbubbles were collected at the site of the magnet and the rest of the solution became clear thus indicating magnetic removal of the bubbles from the solution. The magnetic microbubbles could be freely manipulated along the vial wall with the permanent magnet (Fig. 3e).

Perfluorcarbon Gas-Filled Magnetic Lipid Microbubbles Exhibit Characteristics Desirable for Use in Drug Delivery

To asses if the generated microbubbles exhibit sufficient properties for later use in animals or patients, we accurately checked the properties of every charge of prepared microbubbles. The lipid microbubbles generated from our lipid mixture exhibited strong light scattering properties in the microscope, which is characteristic for the correct formation of gas filled microbubbles. Depending on the lipid mixture, the formed microbubbles exhibit different size distributions. The optimal diameter for use in the circulation is between 2 and 10 µm. A corresponding lipid mixture yielding a sufficient size distribution was chosen for further experimentation (Fig. 4a,b). Gas filled microbubbles readily burst when pressure is applied to the microbubble dispersion. We pressurized freshly prepared microbubbles in a syringe thus proving the nature of the generated constructs as gas filled bubbles with a lipid shell (Fig. 4c, d). To demonstrate the correct integration of iron oxide particles coupled to active ingredients, we chose perylene as a model substance. Perylene is a yellow fluorescing dye witch owns chemical and physical properties similar to rapamycin. As demonstrated by microscopic imaging, perylene coated iron oxide nanoparticles completely bind to the lipid shell of the generated microbubbles (Fig. 4e,f).

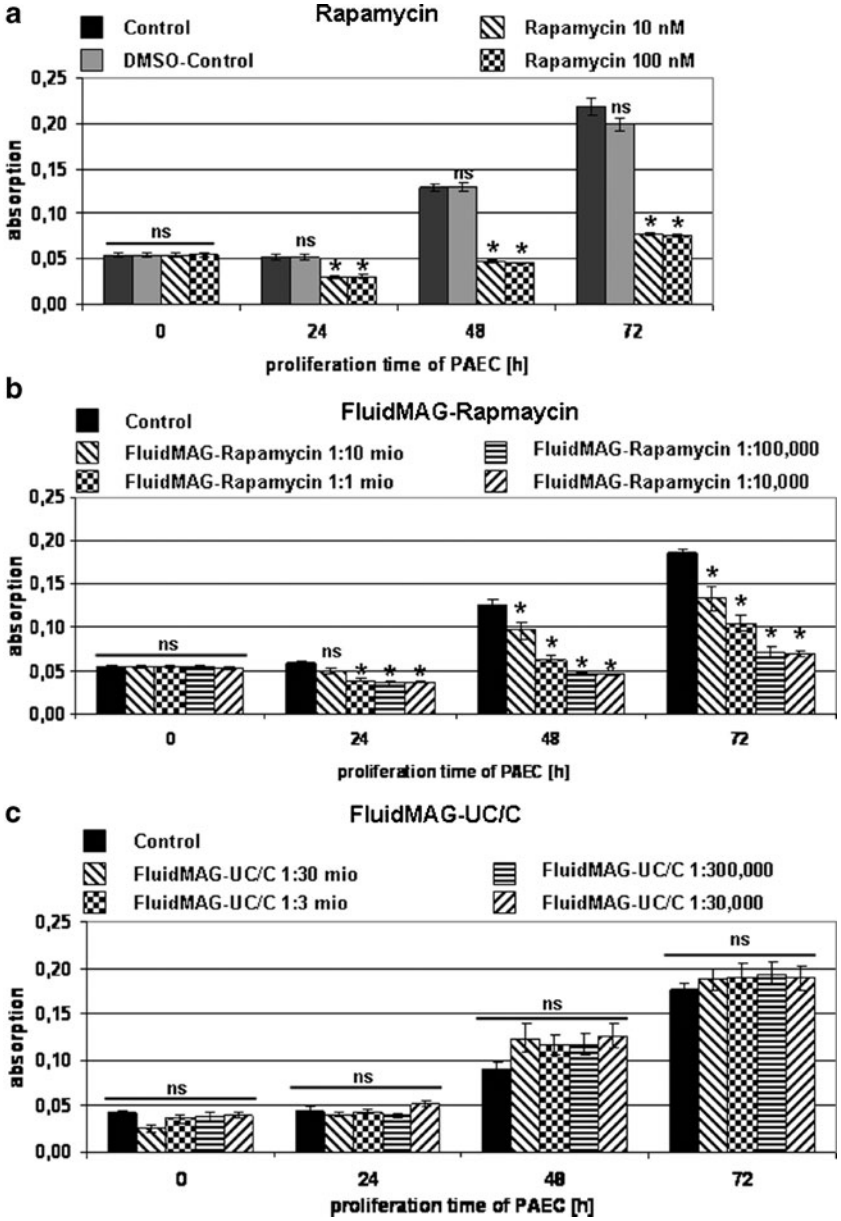

Fig. 1 Rapamycin coupled to superparamagnetic iron oxide nanoparticles inhibits proliferation of porcine aortic endothelial cells. Porcine aortic endothelial cells (PAEC) were treated with rapamycin in a concentration of 10 or 100 nM or with rapamycin-coupled superparamagnetic iron oxide nanoparticles (FluidMAG-Rapamycin) in equimolar concentrations (1:10.000.000 to 1: 10.000) or with similar concentrations of uncoated nanoparticles (FluidMAG-UC/C) for up to 3 days. Cell proliferation was assessed by MTT reduction daily. (**a**) Rapamycin in concentrations of 10 and 100 nM nearly completely inhibited cell proliferation of PAEC. (**b**) Rapamycin coupled to iron oxide nanoparticles also inhibited cell proliferation of PAEC in a dose dependent manner. (**c**) Naked nanoparticles did not influence cell proliferation of PAEC. (Experiments $n=3$ in 8-likates, ns = not significant, *=$p<0,5$ ANOVA/Dunns post-hoc test).

Lipid Microbubbles Carry Drug-Coated Superparamagnetic Iron Oxide Nanoparticles in Circulating Fluids to Target Sites, Can Be Deposited from Flowing Dispersion on Behalf of Magnetizeable Stents and External Magnetic Fields

To test the retention of coated iron oxide nanoparticles bound to microbubbles from flowing fluids, a teflon tube with an inner diameter of 4 mm was stented with a commercially available stent (Coroflex Blue®, 4 mm × 25 mm, BBraun, Melsungen, Germany; Fig. 6a–c). The tube was connected to a peristaltic pump and a dispersion of magnetic microbubbles was circulated through the stented tube (see Fig. 5a,b). The flow velocity was chosen at 5 cm/s comparable to flow circumstances in small human vessels. In a first approach to investigate the behaviour of magnetic material in the system, the retention of dispersed iron oxide nanoparticles which were not incorporated into

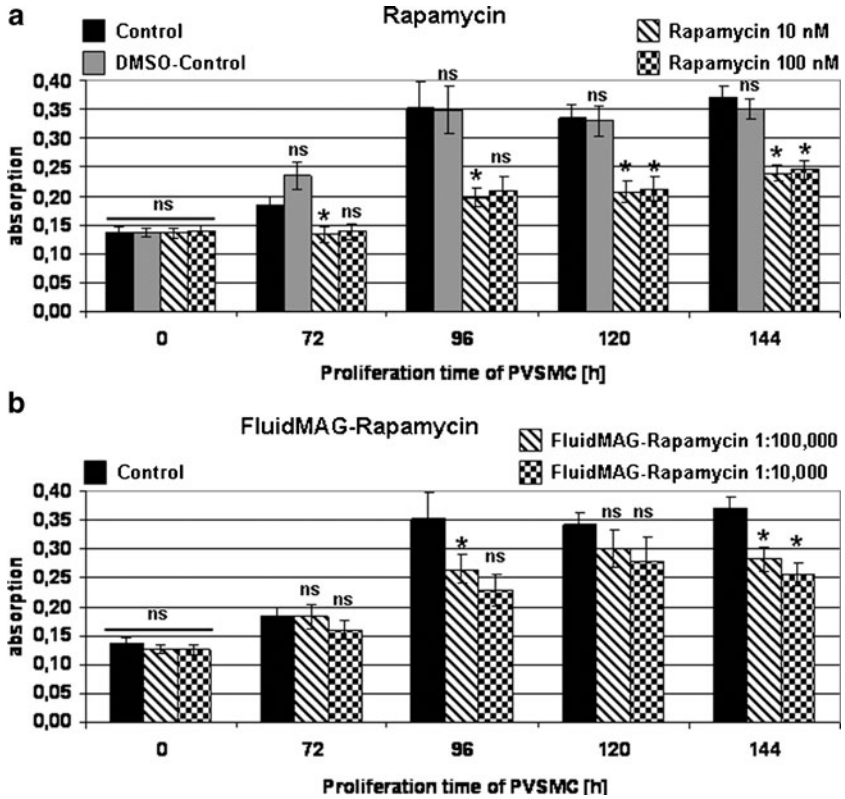

Fig. 2 Rapamycin coupled to superparamagnetic iron oxide nanoparticles inhibits proliferation of porcine vascular smooth muscle cells. Porcine vascular smooth muscle cells (PVSMC) were either treated with rapamycin in a concentration of 10 or 100 nM or with rapamycin-coupled superparamagnetic iron oxide nanoparticles (FluidMAG-Rapamycin) in equimolar concentrations (1:100.000 and 1: 10.000) for up to 6 days. After addition of rapamycin to the cell culture medium cell proliferation was assessed daily by MTT reduction up to 72 h. (**a**) Rapamycin in concentrations of 10 and 100 nM significantly inhibited cell proliferation of PVSMC. (**b**) Equally, rapamycin coupled to iron oxide nanoparticles inhibited proliferation of PVSMC. (Experiments $n=3$ in 4-likates, ns = not significant, *=$p < 0,5$ ANOVA/Bonferonis post test).

microbubbles was investigated. In a tube without a magnetizeable stent, the particles were deposited at the edges of attached solid magnets (Fig. 5c,d). This behaviour fits well to our expectations deduced from physical theories covering magnetism. The deposition was far from being exhaustive. Only a small amount of the applied superparamagnetic particles could be detected at the magnets.

The same behaviour was seen when applying a commercially available stent to the tube, which was not subjected to further treatment. Since commercially available stents are produced from cobalt chromium alloys, which are not magnetic, these stents do not behave as field modulating elements (Fig. 6d,e). Following these first experiments we used a nickel plated original stent (about 10 µm nickel layer thickness) to apply a magnetizeable stent to induce strong field gradients from a homogenous magnetic field realized by external magnets. As seen in Fig. 6f–h, the superparamagnetic particle bearing microbubbles were deposited at the stent struts as intended when using this approach. To detect the particles deposited to the stent struts we used the particles coated with perylene as a model substance for pharmacological active compounds. The deposited particles were then detected by fluorescence microscopic imaging (Fig. 6i,j).

Deposition of Magnetic Material Depends on Circulation Time of Magnetic Microbubbles and Field Force of External Magnetic Field

After deposition of the microbubbles at the stent struts the bubbles could be destroyed by additional application of ultrasound (Fig. 5b). The perylene coated iron oxide nanoparticles remained at the stent struts. After removing the stented tube from the system, the deposited perylene was dissolved from the retained iron oxide particles with methanol, the particles removed by magnetic force and the dissolved dye quantified by photometric measurement at 470 nm (Fig. 7). Thus a quantification of the deposited fraction of the applied iron oxide nanoparticles at the stented site of the tube system was possible.

Under flow we could show that the amount of retained perylene, as a dummy for real drugs, depended on the circulation time of the magnetic microbubbles. As short as 20 min of circulation was sufficient to retain a maximum of

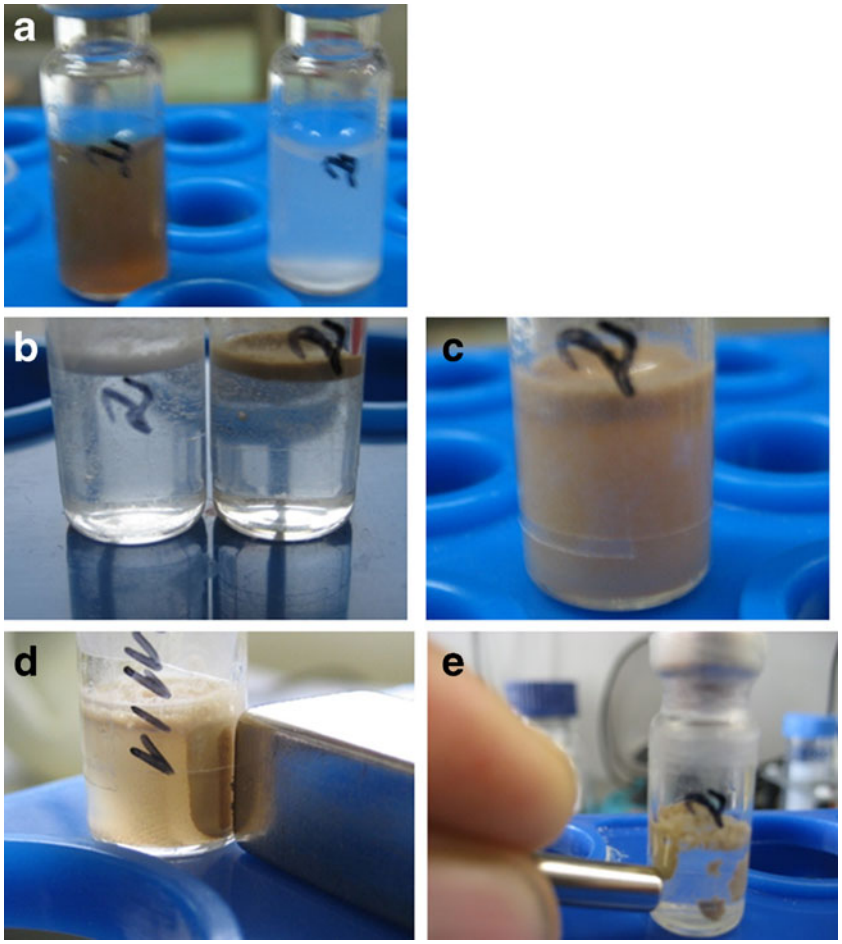

Fig. 3 Synthesis of superparamagnetic iron oxide nanoparticles loaded lipid microbubbles. (**a**) Mixtures of DPPE and DPPC can be suspended with or without magnetic iron oxide nanoparticles in water/10% glycerine and form opaque suspensions. (**b**, **c**) When shaken with perfluorcarbon gas, the lipid suspensions form stable gas filled microbubbles with a lipid shell. The bubbles float from the dispersion after some time but can readily be resuspended by slightly shaking the vial. (**d**, **e**) When superparamagnetic iron oxide nanoparticles are incorporated in the formed microbubbles, the bubbles can be collected at a permanent magnet or manipulated by magnetic force in fluids.

about 60% of the applied material at the stented site of the tube system (Fig. 8b). Longer circulation times did not noteworthy affect the amount of retained material. However, lowering flow velocity led to increased microbubble deposition (data not shown). To investigate the influence of the force of the external magnetic field on the retention of magnetic material at the magnetizeable stents, we quantified the deposition of magnetic material at different distances from the external permanent magnets (Fig. 8a). As expected, with growing distance of the external magnets and subsequent decreasing magnetic field force within the range of the magnetizeable stent, the deposition of magnetic material decreased dramatically (Fig. 8c).

DISCUSSION

We here, for the first time, describe the possibility to use drug coated paramagnetic iron oxide nanoparticles transported by lipid based microbubbles combined with implantable vascular stents that exert magnetic properties for site directed targeting of vasoactive drugs. Deposition of an antirestenotic immunosuppressant drug, namely rapamycin, is reached by i. using magnetic nanoparticles that are complexed to the drug, ii. incorporating them into lipid microbubbles, which are well known to circulate freely within the vasculature, and iii. ultimately retaining them at a magnetizable stent through external application of a distantly placed permanent magnet. This technology could be of a substantial progress in minimally-invasive drug (re-) loading of already implanted vascular stents that develop restenosis, a major limitation of vascular stenting (4). Until now, such treatment commonly requires repeated invasive catheterization procedures with potential additional application of a stent within a stent, accompanied by the well known unwanted side effects and physical as well as psychological impacts on the patient (4).

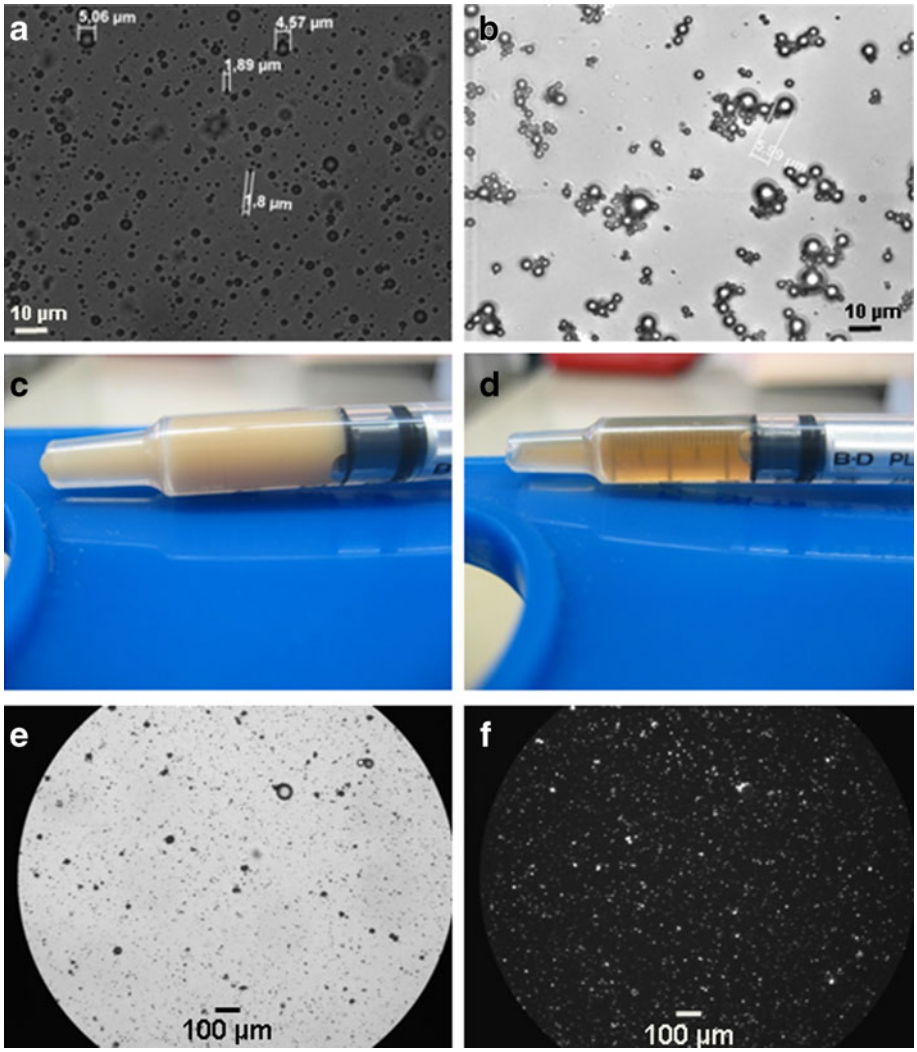

Fig. 4 Characterization of magnetic lipid microbubbles. (**a**, **b**) Prepared lipid microbubbles show strong light scattering characteristics when observed in a light microscope due to the gas filling. The microbubbles exhibit a size distribution between 1,5 and 10 μM. (**c**, **d**) When pressurized in a syringe, correct formed lipid microbubbles burst and leave a clear lipid suspension (**d**) compared to the cloudy suspension (**c**) before pressurization. (**e**, **f**) Nanoparticles coated with the fluorescence dye perylene incorporate into the lipid shell during the formation of the microbubbles. (**e**) Representative microscopic image with transmitting light. (**f**) The same area analyzed by fluorescent imaging demonstrating the localization of the nanoparticles carrying the fluorescence dye in the lipid shell.

Magnetic drug targeting in the vasculature is highly desirable yet complicated by numerous obstacles originating in vascular anatomy and the physiology of blood circulation (13). Among these, one problem is the potential systemic effect of drugs that are delivered via the circulation. Another obstacle – at least within the arterial vasculature – is exerted by the hydrodynamic forces resulting from arterial blood flow velocity. Nonetheless, it is the arterial system, which is affected by many important vascular diseases, such as atherosclerosis, and these take place in arteries or arterioles which exhibit flow velocities of 2–70 cm/s (14). Since magnetic deposition of particles from flowing fluids strongly depends on flow velocity, this has important consequences for the magnetic force needed to retain a substance from flowing blood in arteries. Further problems with vascular drug delivery result from the binding of substances or drug coated carrier constructs to plasma proteins, which also potentially limits the use of ferric oxide nanoparticles to bind drugs for magnetic targeting (15). Additionally, free particles applied to the vasculature may interact with the immune system and thus may be withdrawn from the blood or cause thrombosis.

The incorporation of nanoparticle-bound therapeutic drugs into lipid microbubbles therefore offers several advantages that may overcome the main obstacles: microbubbles of limited size – as the ones produced in this study - are known from the established use as ultrasound contrast agents to circulate freely through the vasculature and to be able to pass the capillary system without causing vascular occlusion (16). Unless they are deployed by ultrasound, they do not release their cargo and thus they offer the possibility to limit systemic side effects. Microbubble-incorporated drugs do not participate in plasma protein binding or agglomeration and thus have a predictable bioavailability and limited deposition at non-target sites. Most importantly, the accumulation of magnetic nanoparticles in a microbubble dramatically increases the magnetic moment exerted on this structure, thus optimizing the likeliness of its magnetic retention even under higher flow rates.

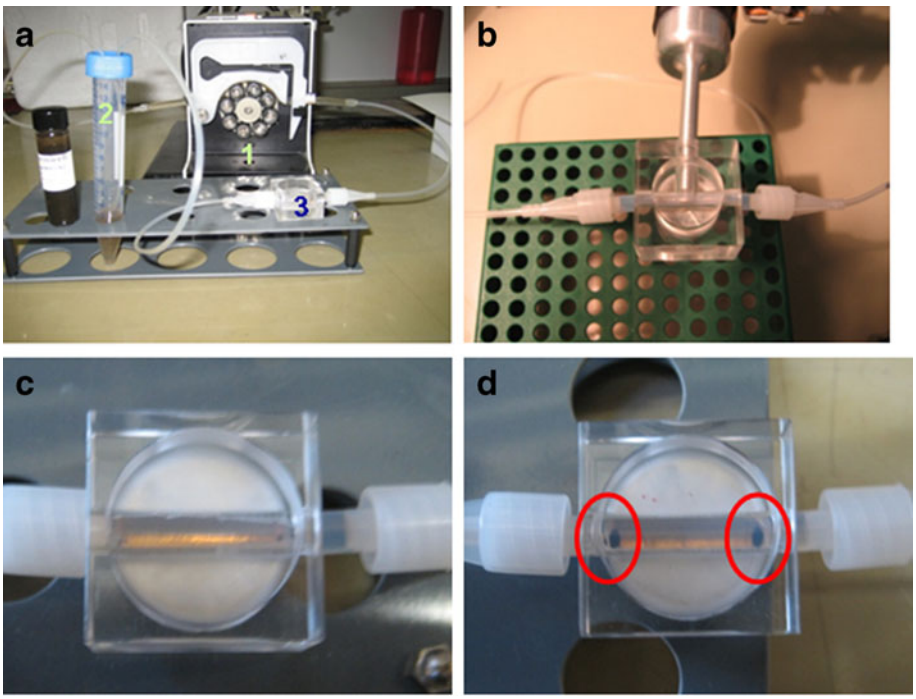

Fig. 5 Experimental setup to assess the deposition of magnetic material in a test tube. (**a**) A Teflon tube (3) is connected via flexible tubes to a peristaltic pump (1) and a fluid reservoir (2). Superparamagnetic iron oxide nanoparticles are filled into the fluid reservoir and circulated through the test tube. (**b**) The test tube is placed into a cube made from acrylic glass with cavities for the reproducible application of permanent magnets in a defined distance. Additionally an ultrasound device can be applied to the test tube to destroy deposited microbubbles at the test site. (**c**) No deposition of magnetic iron oxide nanoparticles can be observed when no field influencing elements are placed within the test tube. (**d**) Superparamagnetic nanoparticles from the circulating fluid are deposited at the edges of the applied magnets (circles) after some time of circulation.

To reach our goal to transport and deposit rapamycin with the help of magnetic nanoparticles it was a prerequisite that the drug once bound to the iron oxide nanoparticles and lipid microbubbles maintained its pharmaceutical activity. Using primary endothelial and vascular smooth muscle cells from porcine aortae (PAEC, PVSMC) we show that the proliferation inhibiting effect of the nanoparticle complexed rapamycin is unaltered when compared with equimolar amounts of uncomplexed Rapamycin. This is of high importance because neointima formation is a process mainly originating from endothelial and vascular smooth muscle cells within a stented area (17,18). We further show that the inhibition of cell proliferation is not a feature of the particles themselves, since iron oxide nanoparticles which do not carry any drug (FluidMAG-UC/C) do not influence cell culture parameters at all. Also these complexes can stably be bound to specifically designed lipid microbubbles. Binding the nanoparticles-drug complexes to our lipid microbubbles yielded in completely magnetically steerable constructs which also allow for their magnetic manipulation in a solution, another prerequisite for our goal of magnetic retention of the complexed drugs from a flowing system. Interestingly, neither rapamycin, nor the model substance perylene influenced the binding of FluidMag particles to the specific lipid bubbles, thus potentially offering the advantage of transporting a wide variety of substances that principally can bind to FluidMag using this technology. However, this was not the goal of our study and therefore, no other drugs were tested at this point. Our bubbles not only effectively bound and transported rapamycin coated nanoparticles, but also showed all biophysical properties of gas filled microbubbles intended to be used in the vasculature (19). They exhibited strong light scattering properties in light microscope and were deployable by pressure and ultrasound. Furthermore, after finding a correct ratio of components for the mixture of our microbubbbles, they showed a stable size distribution between 1 and 10 µm, which is optimal for circulation in the vasculature and complies with commercially offered microbubbles for use as ultrasound contrast agents as compared in microscopic imaging (e.g. Sonovue®) (20,21). The generated microbubbles did not agglutinate in plasma (data not shown) which is an important prerequisite for the use *in vivo*.

In experiments under flow we show that the retention of nanoparticle-bound drugs to a model target site within a tube flowing system is only insufficient when these complexes are not linked to microbubbles. This reflects the physical fact that magnetic retainability of particles from a flowing liquid is largely dependent on the size of these particles and their resulting magnetic moment, which, in the case of nanoparticles is extremely low (22). However, as shown by the same experiments, complexing numerous

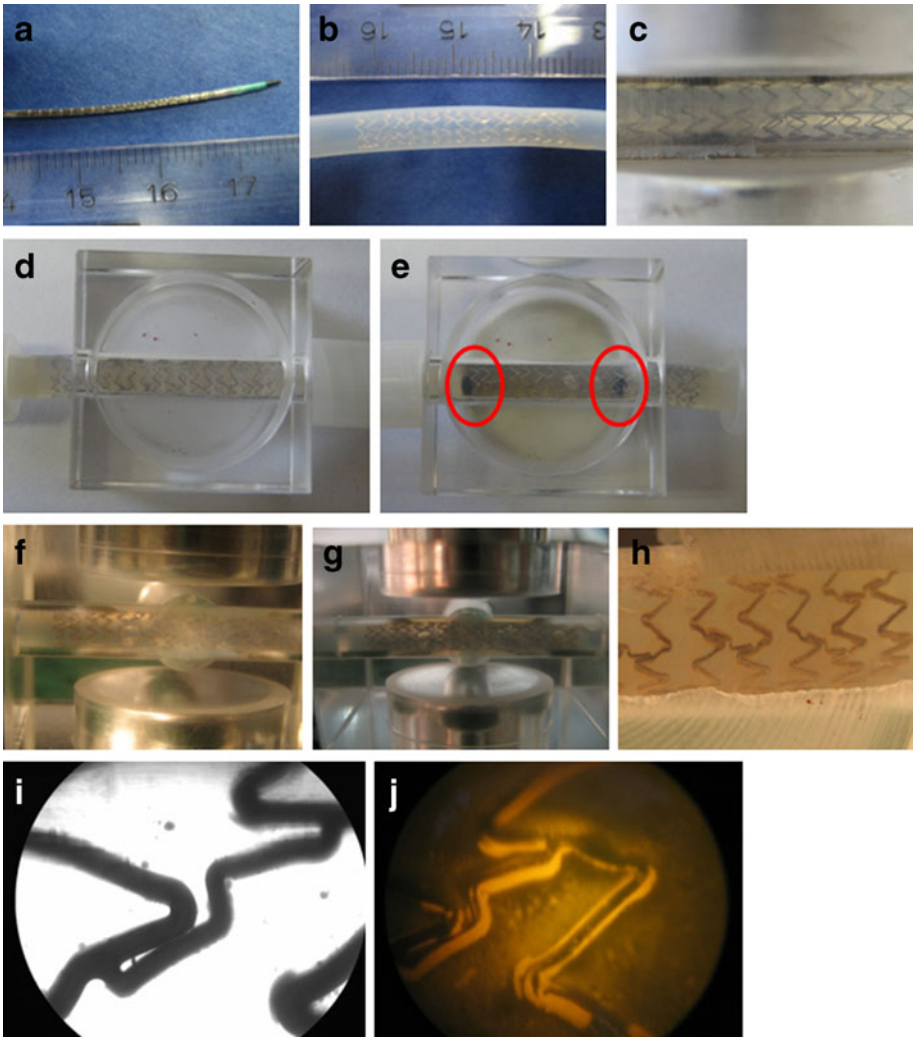

Fig. 6 Superparamagnetic iron oxide nanoparticles loaded with drugs or model substances are deposited at a magnetized commercial stent. (**a**,**b**) A commercially available coronary stent (Coroflex Blue, 4 × 25 mm, BBraun) is placed into a teflon test tube by balloon expansion. After stenting the test tube, microbubbles loaded with magnetic iron oxide nanoparticles are circulated through the experimental setup and subsequently destroyed by ultrasound application. (**c**) Detail of stent struts of the expanded stent in the tube. (**d**, **e**), Magnetic microbubbles are deposited at the edge of the applied magnets when using a non magnetisable stent similar to the situation when no stent is present. (**f**, **g**) The stent is made magnetizeable by nickel plating resulting in deposition of magnetic microbubbles at the stent struts. (**h**) Details of stent struts thickly covered with deposited microbubbles. (**i**) Microphotograph of stent struts after the destruction of the captured microbubbles by ultrasound at a magnification of 100 fold. (**j**) The same stent struts in fluorescent microscope imaging. As can be seen, the perylene coated iron oxide nanoparticles (yellow fluorescence) are readily deposited at the stent struts.

particles in microbubbles and thus artificially increasing the magnetic moment of the resulting constructs that are to be retained can overcome this problem. Of note, for our fluorescent experiments, it was not possible to use rapamycin, as this substance does not exhibit fluorescence properties and a chemical fluorescent modification would not possess the same binding properties as rapamycin does. As it was desirable to visualize the deposited nanoparticles in a microscope, we used a fluorescence dye (perylene) with chemical and physical binding properties almost identical to rapamycin. When we incorporated a magnetizable stent within the flow tube system, we dramatically enhanced the retention of the microbubbles at the target site and directed the deposited material right to the struts of the stent. This step was an important prerequisite for our ultimate goal of "reloading" a stent with bioactive nanoparticle-bound rapamycin. Most importantly, however, this stent actually allows for dramatically increasing the distance of the external magnet from the target site within the flow-through system by creating strong magnetic field gradients in the proximity of the stent struts. Of note, the method for magnetizing the stent that we used in this pilot study may not be ideal for *in vivo* use, as nickel is known to be allergenic and also may raise concerns about the *in vivo* fate of the nickel coating. However, the concept of magnetizeable stents has previously been used successfully to deliver nanoparticle loaden cells to stents of 304 stainless steel, too, which were also magnetic, and may not cause these problems (10,11,23). This trick may

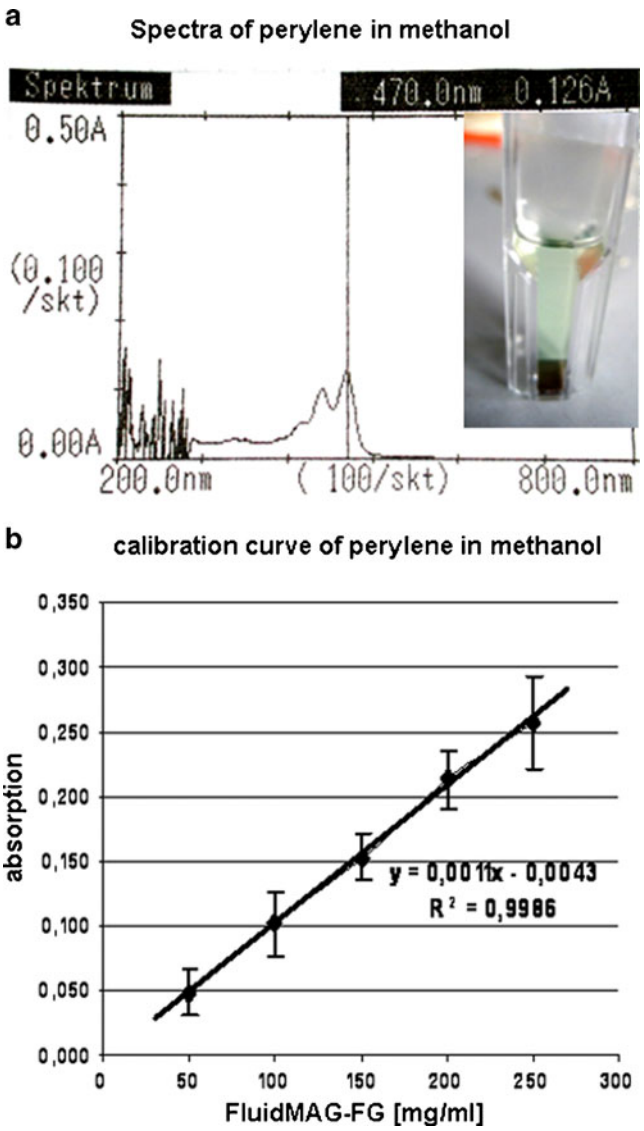

Fig. 7 Perylene loaded iron oxide nanoparticles can be quantified by solving the perylene in methanol and subsequent spectrophotometric measurement. (**a**) Representative spectrum of perylene resolved from FluidMAG-FG particles. (**b**) Calibration curve of perylene in methanol after resolving it from FluidMAG-FG particles in different concentrations.

ultimately overcome the limitations of low tissue penetration of external magnetic fields and additionally dramatically improve site directed deposition, since the magnetic field gradient essential for particle deposition is only strong enough in the close proximity of the magnetic stent. Without magnetic stent, no particle deposition takes place at greater distances of the applied permanent magnets (data not shown).

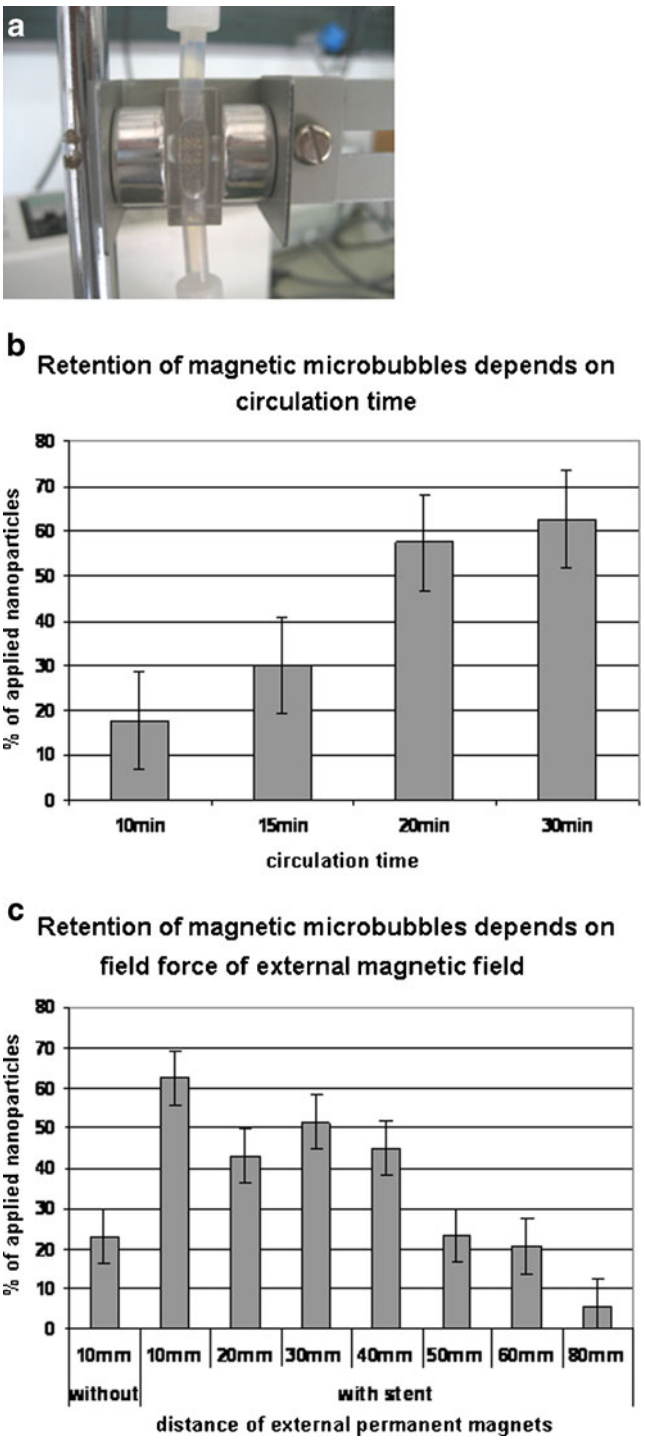

Fig. 8 Influence of circulation time and magnetic field force on retention of magnetic microbubbles at magnetizable stents. (**a**) Experimental setup to assess the dependency of the deposition of magnetic microbubbles at magnetizable stent struts in dependence of the distance of the externally placed permanent magnets. (**b**) The deposited amount of magnetic microbubbles is dependent on circulation time at a constant circulation velocity. After about 20 min, the maximum of bubble deposition is reached. Further circulating magnetic microbubbles does not increase the amount of deposited material. At 5 cm/s fluid velocity, a maximum of 60% of the deployed iron oxide nanoparticles could be recovered at the stented site of the test tube ($n=3$). (**c**) With increasing distances of the external permanent magnets and subsequent decreasing magnetic field forces the deposition of magnetic microbubbles is reduced. When the external magnets are placed 80 mm apart, less than 10% of the deployed iron oxide nanoparticles are recovered at the stented tube site after circulation and subsequent destruction by ultrasound.

Besides the great efforts made in this project, there are still some minor potential limitations of our technology for application in humans. First, to magnetize the stent, it was plated by nickel, a substance with good biocompatibility at low amounts as previously shown in stent technology (24). However, as mentioned above, nickel potentially causes allergic reactions. Therefore, the long term strategy pursued by us is to replace the nickel plating process by the use of a per se magnetic alloy to produce the stents. A known alloy with sufficient properties for the use in humans is 304 stainless steel. In following investigations stents cut from different magnetic alloys should be examined about their magnetic and mechanic properties and optimized for the use in this drug delivery system. Second, magnetizeable stents may be dislocated when exposed to a strong magnetic field, e.g. when a patient with a magnetizeable stent would undergo magnetic resonance imaging (MRI) or may heat up when exposed to an alternating magnetic field. However, results from previous studies using similar stents in MRI, do not give any evidence for adverse reactions (25). The behaviour of magnetisable stents in magnetic fields has to be characterized carefully before using them in patients. A second topic is the fate of the iron oxide particles not sequestered to the magnetized stent and the fate of the drug loaded iron oxide nanoparticles once set free from the lipid microbubbles by ultra sound application at the magnetized stent. Iron oxide nanoparticles are known to be cleared from the blood by the reticoendothelial system and subsequently accumulate in the spleen and the liver. Accumulation of drugs coated to the particles in these organs may cause unwanted side effects. Thus, besides a nearly quantitative capture of nanoparticles loaded microbubbles it is necessary to realize a stable binding of the deposited material at the target site, e. g. by an additionally functionalized coating, after the external magnets are removed. The drug carrying particles thus will form a depot of therapeutic agents at the stented site, too. Mechanisms potentially useful to realize such interactions between particles and the vessel wall may include antigene-antibody reactions or the reaction of integrines with RGD peptides Also, the naturally occurring accumulation of ironoxide particles in atherosclerotic plaques due to their incorporation into phagocytes assembling in restenosed vessel walls can be used (26). The advancement of the technology to overcome these limitations is already topic of our further investigations.

CONCLUSION

In conclusion, we here present for the first time a working drug delivery system for the site directed targeting of antiproliferative drugs to restenoses in already implanted vascular stents. In comparison to previously described approaches, the incorporation of drug loaded nanoparticles into lipid based microbubbles may overcome the disadvantages of solid carrier systems combining high magnetic moments with the flexibility of lipid microbubbles.

Our demonstrated drug targeting system exhibits the potential to reduce the burden of high risk combined with repeated intervention from patients and concomitantly allows for individualization of mode and period of drug therapy, thus leading the way to a more contemporary therapy of cardiovascular lesions.

REFERENCES

1. Fischman DL, Leon MB, Baim DS, Schatz RA, Savage MP, Penn I, Detre K, Veltri L, Ricci D, Nobuyoshi M. A randomized comparison of coronary-stent placement and balloon angioplasty in the treatment of coronary artery disease. Stent Restenosis Study Investigators. N Engl J Med. 1994;331:496–501.
2. Serruys PW, de Jaegere P, Kiemeneij F, Macaya C, Rutsch W, Heyndrickx G, Emanuelsson H, Marco J, Legrand V, Materne P. A comparison of balloon-expandable-stent implantation with balloon angioplasty in patients with coronary artery disease. Benestent Study Group. N Engl J Med. 1994;331:489–95.
3. Daemen J, Serruys PW. Drug-eluting stent update 2007: part I. A survey of current and future generation drug-eluting stents: meaningful advances or more of the same? Circulation. 2007;116:316–28.
4. Dangas GD, Claessen BE, Caixeta A, Sanidas EA, Mintz GS, Mehran R. In-stent restenosis in the drug-eluting stent era. J Am Coll Cardiol. 2010;56:1897–907.
5. Grewe PH, Deneke T, Machraoui A, Barmeyer J, Muller KM. Acute and chronic tissue response to coronary stent implantation: pathologic findings in human specimen. J Am Coll Cardiol. 2000;35:157–63.
6. Joner M, Finn AV, Farb A, Mont EK, Kolodgie FD, Ladich E, Kutys R, Skorija K, Gold HK, Virmani R. Pathology of drug-eluting stents in humans: delayed healing and late thrombotic risk. J Am Coll Cardiol. 2006;48:193–202.
7. Finn AV, Nakazawa G, Joner M, Kolodgie FD, Mont EK, Gold HK, Virmani R. Vascular responses to drug eluting stents: importance of delayed healing. Arterioscler Thromb Vasc Biol. 2007;27:1500–10.
8. Scheller B, Hehrlein C, Bocksch W, Rutsch W, Haghi D, Dietz U, Bohm M, Speck U. Treatment of coronary in-stent restenosis with a paclitaxel-coated balloon catheter. N Engl J Med. 2006;355:2113–24.
9. Unverdorben M, Vallbracht C, Cremers B, Heuer H, Hengstenberg C, Maikowski C, Werner GS, Antoni D, Kleber FX, Bocksch W, Leschke M, Ackermann H, Boxberger M, Speck U, Degenhardt R, Scheller B. Paclitaxel-coated balloon catheter *versus* paclitaxel-coated stent for the treatment of coronary in-stent restenosis. Circulation. 2009;119:2986–94.
10. Pislaru SV, Harbuzariu A, Gulati R, Witt T, Sandhu NP, Simari RD, Sandhu GS. Magnetically targeted endothelial cell localization in stented vessels. J Am Coll Cardiol. 2006;48:1839–45.
11. Chorny M, Fishbein I, Yellen BB, Alferiev IS, Bakay M, Ganta S, Adamo R, Amiji M, Friedman G, Levy RJ. Targeting stents with local delivery of paclitaxel-loaded magnetic nanoparticles using uniform fields. Proc Natl Acad Sci U S A. 2010;107:8346–51.
12. Mannell H, Hammitzsch A, Mettler R, Pohl U, Krotz F. Suppression of DNA-PKcs enhances FGF-2 dependent human endothelial

cell proliferation via negative regulation of Akt. Cell Signal. 2010;22:88–96.
13. Slevin M, Badimon L, Grau-Olivares M, Ramis M, Sendra J, Morrison M, Krupinski J. Combining nanotechnology with current biomedical knowledge for the vascular imaging and treatment of atherosclerosis. Mol Biosyst. 2010;6:444–50.
14. Ross R. Atherosclerosis–an inflammatory disease. N Engl J Med. 1999;340:115–26.
15. Peng ZG, Hidajat K, Uddin MS. Adsorption of bovine serum albumin on nanosized magnetic particles. J Colloid Interface Sci. 2004;271:277–83.
16. Lindner JR, Song J, Jayaweera AR, Sklenar J, Kaul S. Microvascular rheology of Definity microbubbles after intra-arterial and intravenous administration. J Am Soc Echocardiogr. 2002;15:396–403.
17. Ferns GA, Avades TY. The mechanisms of coronary restenosis: insights from experimental models. Int J Exp Pathol. 2000;81:63–88.
18. Schiele TM, Krotz F, Klauss V. Vascular restenosis - striving for therapy. Expert Opin Pharmacother. 2004;5:2221–32.
19. Unger EC, Porter T, Culp W, Labell R, Matsunaga T, Zutshi R. Therapeutic applications of lipid-coated microbubbles. Adv Drug Deliv Rev. 2004;56:1291–314.
20. Braide M, Rasmussen H, Albrektsson A, Bagge U. Microvascular behavior and effects of sonazoid microbubbles in the cremaster muscle of rats after local administration. J Ultrasound Med. 2006;25:883–90.
21. Grishenkov D, Kari L, Brodin LK, Brismar TB, Paradossi G. In vitro contrast-enhanced ultrasound measurements of capillary microcirculation: comparison between polymer- and phospholipid-shelled microbubbles. Ultrasonics. 2011;51:40–8.
22. Chertok B, Moffat BA, David AE, Yu F, Bergemann C, Ross BD, Yang VC. Iron oxide nanoparticles as a drug delivery vehicle for MRI monitored magnetic targeting of brain tumors. Biomaterials. 2008;29:487–96.
23. Polyak B, Fishbein I, Chorny M, Alferiev I, Williams D, Yellen B, Friedman G, Levy RJ. High field gradient targeting of magnetic nanoparticle-loaded endothelial cells to the surfaces of steel stents. Proc Natl Acad Sci U S A. 2008;105:698–703.
24. Holton A, Walsh E, Anayiotos A, Pohost G, Venugopalan R. Comparative MRI compatibility of 316 L stainless steel alloy and nickel-titanium alloy stents. J Cardiovasc Magn Reson. 2002;4:423–30.
25. Hug J, Nagel E, Bornstedt A, Schnackenburg B, Oswald H, Fleck E. Coronary arterial stents: safety and artifacts during MR imaging. Radiology. 2000;216:781–7.
26. Uppal R, Caravan P. Targeted probes for cardiovascular MR imaging. Future Med Chem. 2010;2(3):451–70.